EARTHQUAKE ENGINEERING AND STRUCTURAL DYNAMICS
Earthquake Engng Struct. Dyn. 2001; **30**:1769–1789 (DOI: 10.1002/eqe.92)

Comparing response of SDF systems to near-fault and far-fault earthquake motions in the context of spectral regions

Anil K. Chopra*,† and Chatpan Chintanapakdee

Department of Civil and Environmental Engineering, University of California, Berkeley, CA 94720, U.S.A.

SUMMARY

In spite of important differences in structural response to near-fault and far-fault ground motions, this paper aims at extending well-known concepts and results, based on elastic and inelastic response spectra for far-fault motions, to near-fault motions. Compared are certain aspects of the response of elastic and inelastic SDF systems to the two types of motions in the context of the acceleration-, velocity-, and displacement-sensitive regions of the response spectrum, leading to the following conclusions. (1) The velocity-sensitive region for near-fault motions is much narrower, and the acceleration-sensitive and displacement-sensitive regions are much wider, compared to far-fault motions; the narrower velocity-sensitive region is shifted to longer periods. (2) Although, for the same ductility factor, near-fault ground motions impose a larger strength demand than far-fault motions—both demands expressed as a fraction of their respective elastic demands—the strength reduction factors R_y for the two types of motions are similar over corresponding spectral regions. (3) Similarly, the ratio u_m/u_0 of deformations of inelastic and elastic systems are similar for the two types of motions over corresponding spectral regions. (4) Design equations for R_y (and for u_m/u_0) should explicitly recognize spectral regions so that the same equations apply to various classes of ground motions as long as the appropriate values of T_a, T_b and T_c are used. (5) The Veletsos–Newmark design equations with $T_a = 0.04$ s, $T_b = 0.35$ s, and $T_c = 0.79$ s are equally valid for the fault-normal component of near-fault ground motions. Copyright © 2001 John Wiley & Sons, Ltd.

KEY WORDS: near-fault records; deformation ratio; deformation response spectra: elastic and inelastic; spectral regions; strength reduction factor

INTRODUCTION

Ground motions recorded within the near-fault region of an earthquake at stations located toward the direction of the fault rupture are qualitatively quite different from the usual

* Correspondence to: Anil K. Chopra, 707 Davis Hall, Department of Civil and Environmental Engineering, University of California, Berkeley, CA, 94720, U.S.A.
† E-mail: chopra@ce.berkeley.edu

Contract/grant sponsor: National Science Foundation; Contract/grant number: CMS-9812531

Received 23 October 2000
Revised 17 February 2001
Accepted 19 March 2001

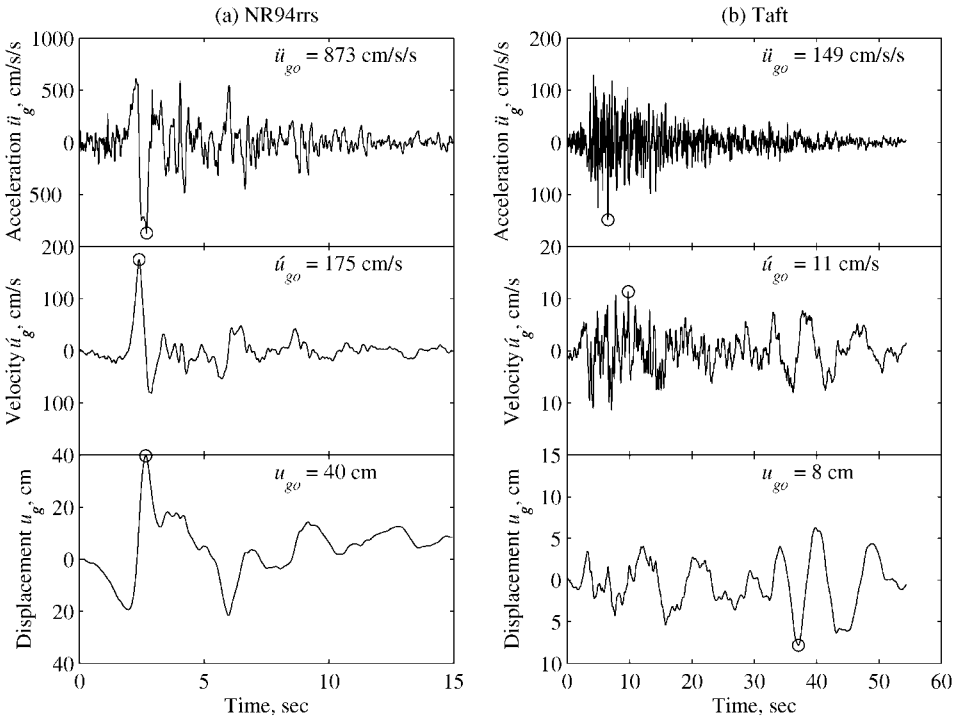

Figure 1. Fault-normal component of ground motions recorded at (a) Rinaldi Receiving Station, 1994 Northridge earthquake and (b) Taft, 1952 Kern County earthquake.

far-fault earthquake ground motions. The fault-normal component of a ground motion recorded in the near-fault region of the Northridge, California, earthquake of 17 January 1994 displays a long-period pulse in the acceleration history that appears as a coherent pulse in the velocity and displacement histories (Figure 1(a)). Such a pronounced pulse does not exist in ground motions recorded at locations away from the near-fault region, e.g. the Taft record obtained from the Kern County, California, earthquake of 21 July 1952 (Figure 1(b)).

Because of the unique characteristics of near-fault ground motion, structural response to near-fault ground motions has received much attention in recent years. The very large deformation demands on fixed-base buildings [1–3] and base-isolated buildings [3] have been of special concern. Inelastic response of buildings to pulse-type motions have been investigated with the objective of incorporating the special response features in the design process [4]. The strength reduction factors and ratio of peak deformations of inelastic and corresponding elastic systems have been investigated [5]. Validity of the capacity spectrum method to estimate structural deformations due to near-fault ground motions has also been examined [5]. The drift demand spectrum has been proposed as a new measure of earthquake demand imposed by near-fault ground motion [6]. Most of the investigations cited above emphasize the differences in structural response to near-fault ground motions—containing one or more dominant pulses—and far-fault ground motions—which are typically broad-frequency-band excitations.

In spite of these differences it should be possible to extend the well-known fundamental results and concepts about the earthquake response of structures to near-fault ground motions [7]. Towards this objective, the discussion below compares certain aspects of the response of SDF systems to near-fault ground motions with their response to far-fault ground motions. First, we compare the elastic response spectra of the two types of motions, in the context of the acceleration-, velocity-, and displacement-sensitive regions of the response spectrum. Next, we analyse the response of inelastic systems, in particular, the strength reduction factor, R_y, and the ratio u_m/u_0 of deformations of inelastic and elastic systems in the context of spectral regions; with emphasis on the acceleration-sensitive region. Finally, we test the validity of existing design equations for R_y and u_m/u_0 for near-fault motions.

GROUND MOTION DATA

The set of 15 ground motions used in this study are listed in Table I. These records are from the near-fault regions of Imperial Valley (1979), Morgan Hill (1984), Loma Prieta (1989), Erzincan (1992), Northridge (1994), and Kobe (1995) earthquakes. For the fault-normal component of each record the peak ground acceleration, $\ddot{u}_{go}$, the peak ground velocity, $\dot{u}_{go}$, and the peak ground displacement, u_{go}, are listed, together with ratios $\dot{u}_{go}/\ddot{u}_{go}$ and $u_{go}/\dot{u}_{go}$. Included for comparison are data for the fault-normal component of the motion recorded at Taft distant from the near-fault region during the Kern County earthquake (1952). The spectral regions and the spectral amplification factors, also shown in Table I, will be discussed in the next section.

This investigation emphasizes the elastic and inelastic response spectrum of the fault-normal component of the selected records because it is known to be more intense than the fault-parallel component. However, limited result will be presented for the fault-parallel component of the two records shown in Figure 2 for comparison.

To compare structural responses to near-fault and far-fault ground motions, we considered the set of 15 records of far-fault motion in Table II, which includes ground motions recorded on rock and firm soil sites during nine different earthquakes that occurred in California and Washington between 1934 and 1983. The earthquakes range in magnitude from 5.7 to 7.7. The epicentral distances of the recording stations range from 12 to 64 km [8].

ELASTIC RESPONSE SPECTRA

Figure 3 shows three elastic response spectra—pseudo-acceleration, A, pseudo-velocity, V and deformation, D—for both fault-normal and fault-parallel components of a near-fault ground motion and a far-fault ground motion. The response spectra for the two components of the NR94rrs record, a near-fault ground motion, are very different. In particular, the fault-normal component imposes a much larger deformation demand and strength demand, $f_s = (A/g)w$, where w is the weight of the SDF system, over a wide range of vibration periods. This is characteristic of most ground motions recorded in the near-fault region of earthquakes; it is a manifestation of the directivity effect that causes the fault-normal component of a near-fault ground motion to be much more intense than the fault-parallel component [9]. In contrast, the elastic response spectra for two components of the Taft ground motion, a far-fault

Table I. Ground motion parameters, spectral regions, and amplification factors of the fault-normal component.

No.	Record	Earthquake	Station	Fault distance (km)	$\ddot{u}_{go}$ (cm/s^2)	$\dot{u}_{go}$ (cm/s)	u_{go} (cm)	$\dot{u}_{go}/\ddot{u}_{go}$	$u_{go}/\dot{u}_{go}$	T_b (s)	T_c (s)	T_d (s)	α_A	α_V	α_D
1	LP89lgpc	Loma Prieta	Los Gatos	3.5	704	173	65	0.25	0.38	0.43	0.79	3.72	3.33	1.71	2.68
2	LP89lex	Loma Prieta	Lexington Dam	6.3	673	179	57	0.27	0.32	0.65	1.09	1.56	2.96	1.94	1.51
3	KB95tato	Hyogo-Ken-Nanbu	Takatori Station	4.3	771	174	56	0.23	0.32	0.70	1.54	1.65	2.15	2.51	1.91
4	KB95kobj	Hyogo-Ken-Nanbu	Kobe Station	3.4	1067	160	40	0.15	0.25	0.35	1.00	1.18	2.35	2.50	1.88
5	KB95kpi1	Hyogo-Ken-Nanbu	Port Island	6.6	426	100	50	0.24	0.50	0.50	1.32	2.80	2.26	2.02	1.81
6	EZ92erzi	Erzincan	Erzincan Station	2.0	424	119	42	0.28	0.35	0.20	1.30	2.47	2.03	1.49	1.66
7	NR94rrs	Northridge	Rinaldi Receiving Station	7.5	873	175	40	0.20	0.23	0.30	0.99	1.21	2.21	1.74	1.50
8	NR94spva	Northridge	Sepulveda	8.9	715	63	16	0.09	0.26	0.13	0.35	2.82	2.55	1.64	2.88
9	NR94sylm	Northridge	Sylmar County Hospital	6.4	718	122	31	0.17	0.25	0.18	0.59	3.23	2.09	1.16	2.34
10	NR94scs	Northridge	Sylmar Converter Station	?	577	131	65	0.23	0.50	0.50	0.89	3.33	2.70	1.69	1.80
11	NR94newh	Northridge	Newhall, LA County Fire Station	7.1	709	119	34	0.17	0.29	0.20	0.75	1.33	2.53	1.80	1.33
12	IV79melo	Imperial Valley	Meloland	0.0	372	117	44	0.32	0.37	0.30	1.89	3.14	1.78	1.70	2.28
13	IV79ar06	Imperial Valley	El Centro Array 6	1.2	424	110	58	0.26	0.53	0.07	1.63	4.46	1.60	1.60	2.16
14	MH84clyd	Morgan Hill	Coyote Dam	0.1	712	70	10	0.10	0.15	0.22	0.58	0.86	2.29	3.17	2.02
15	MH84andd	Morgan Hill	Anderson Dam	4.5	436	27	4	0.06	0.14	0.16	0.40	0.56	1.81	2.66	1.20
	Taft	Kern County		43	149	11	8	0.08	0.69	0.17	0.39	6.06	2.68	2.16	3.03

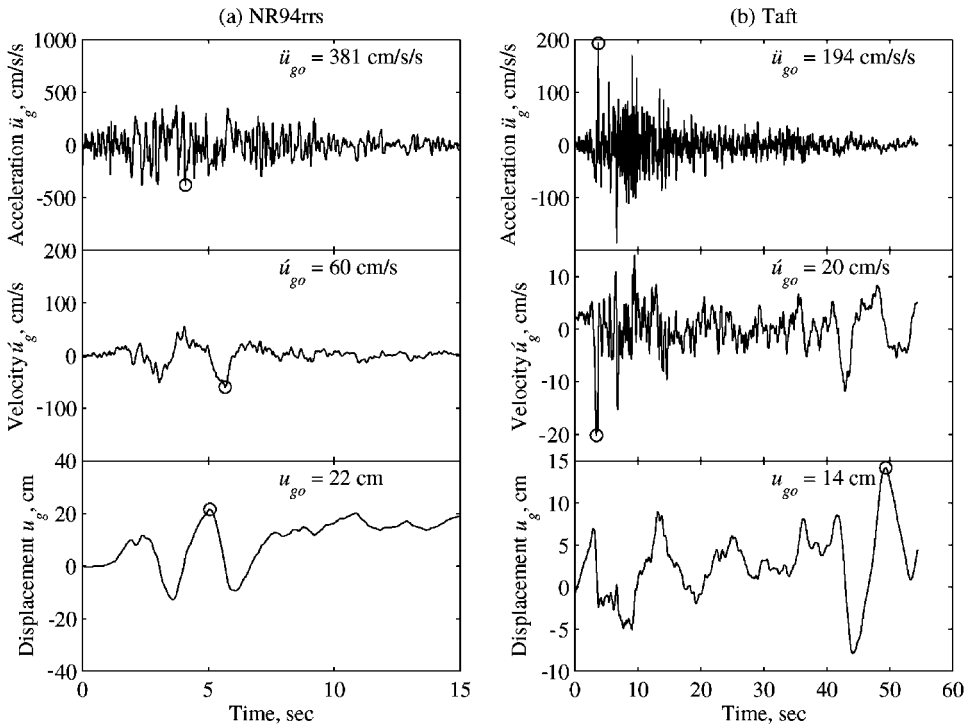

Figure 2. Fault-parallel component of ground motions recorded at (a) Rinaldi Receiving Station, 1994 Northridge earthquake and (b) Taft, 1952 Kern County earthquake.

record, are quite similar over a wide range of vibration periods. The preceding observation from the elastic response spectra for the NR94rrs ground motion is not valid for all near-fault ground motions, however; e.g. the fault-parallel component of the MH84andd record imposes larger strength and deformation demands over a wide range of periods than its fault-normal component (Figure 4).

The strength and deformation demands of the fault-normal component of most near-fault ground motions are much larger than of the fault-parallel component primarily because the former has much larger peak ground acceleration $\ddot{u}_{go}$, velocity $\dot{u}_{go}$ and displacement u_{go}—e.g. $\ddot{u}_{go} = 873$ v s 381 cm/s^2, $\dot{u}_{go} = 175$ v s 60 cm/s^2, and $u_{go} = 40$ v s 22 cm for the NR94rrs record (Figures 1(a) and 2(a))—although its response amplification factors are smaller. This is demonstrated by plotting the response spectra of Figure 3 in normalized form (see Figure 5), where the pseudo-acceleration, pseudo-velocity, and deformation response spectra have been normalized relative to the peak ground acceleration, velocity, and displacement, respectively. Note that the normalized spectrum, which can be interpreted as a response amplification factor, for the fault-normal component is generally smaller than that for the fault-parallel component (Figure 5(a)), although the actual spectrum is larger (Figure 3(a)).

To understand the underlying reason, we examine the normalized response spectrum of Figure 6(b) for the idealized ground motion shown in Figure 6(a), containing n cycles of

Table II. Ground motion parameters of the far-fault ground motions.

No.	Station	Component	Earthquake	Year	M	e (km)	Duration (s)	$\ddot{u}_{go}$ (cm/s^2)	$\dot{u}_{go}$ (cm/s)	$\dot{u}_{go}/\ddot{u}_{go}$
1	Taft	021	Kern county	1952	7.7	43	11.2	152.7	15.7	0.10
2	Taft	111	Kern county	1952	7.7	43	12.6	175.9	17.7	0.10
3	El Centro	000	Lower California	1934	6.5	64	13.0	156.8	20.5	0.13
4	El Centro	090	Lower California	1934	6.5	64	15.6	179.1	11.5	0.06
5	Olympia	176	Western Washington	1949	7.0	16	19.8	161.6	21.4	0.13
6	Olympia	266	Western Washington	1949	7.0	16	19.2	274.6	17.0	0.06
7	Olympia	266	Puget Sound	1965	6.5	61	11.2	194.3	12.7	0.07
8	Castaic	291	San Fernando	1971	6.6	29	15.1	265.4	27.2	0.10
9	Public Utility	180	Long Beach	1933	6.3	27	5.6	192.7	29.3	0.15
10	Public Utility	270	Long Beach	1933	6.3	27	6.4	156.0	15.8	0.10
11	Holtville	225	Imperial Valley	1979	6.6	19	6.7	246.2	44.0	0.18
12	Calexico	225	Imperial Valley	1979	6.6	15	10.9	269.6	18.3	0.07
13	San Yasidro	360	Coyote Lake	1979	5.7	12	7.9	246.2	32.9	0.13
14	San Yasidro	270	Coyote Lake	1979	5.7	12	6.4	228.1	24.9	0.11
15	Parkfield	000	Coalinga	1983	6.5	39	8.2	178.7	14.7	0.08

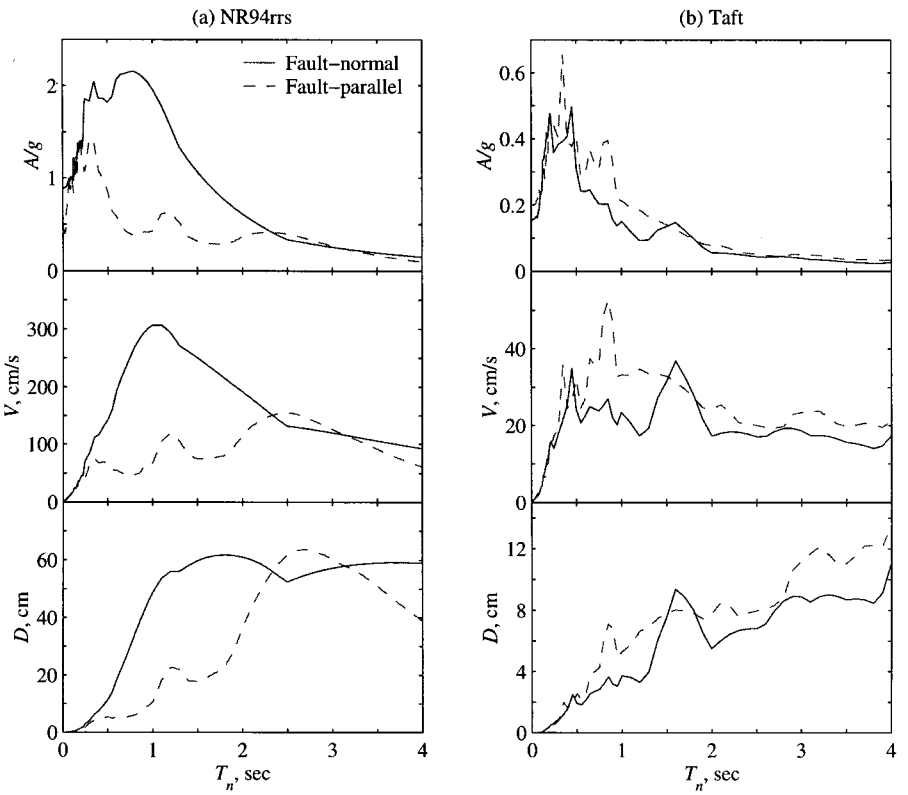

Figure 3. Response spectra for fault-normal and fault-parallel components of (a) NR94rrs and (b) Taft ground motions; damping ratio = 5 per cent.

motion; $n = 1, 2, 3$ and 4. The amplification factors increase with the number of cycles of ground motion, suggesting that the amplification factor for the fault-normal component of the NR94rrs ground motion is smaller because it is dominated by one cycle of large ground velocity, whereas the fault-parallel component contains two large cycles. In contrast, the amplification factors shown in Figure 5(b) are similar for both components of the Taft ground motion, which contain a broad band of frequencies (Figures 1(b) and 2(b)).

Next, we investigate the acceleration-sensitive, velocity-sensitive, and displacement-sensitive regions of the response spectrum. The response spectra for the fault-normal component of Taft and NR94rrs records are presented in Figure 7 as a four-way logarithmic plot using normalized scales $A/\ddot{u}_{go}$, $V/\dot{u}_{go}$, and D/u_{go}. The idealized version of the response spectrum—shown in dashed lines—was constructed according to the procedure described in Reference [10], where the spectrum is divided logically into three period ranges [11, Section 6.8]. The long-period region to the right of point d, $T_n > T_d$, is called the displacement-sensitive region; the short-period region to the left of point c, $T_n < T_c$, is called the acceleration-sensitive region, and the intermediate-period region between points c and d, $T_c < T_n < T_d$, is called the velocity-sensitive region. For a particular ground motion, the periods T_a, T_b, T_e, and T_f on the idealized

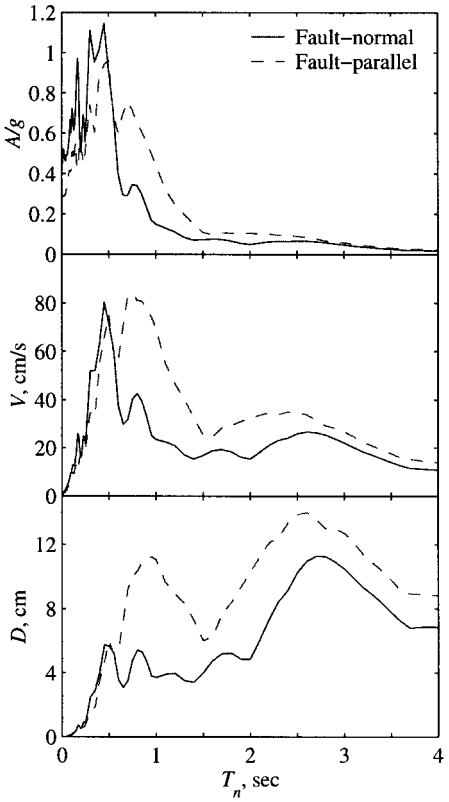

Figure 4. Response spectra for fault-normal and fault-parallel components of MH84andd ground motion; damping ratio = 5 per cent.

spectrum are independent of damping, but T_c and T_d vary with damping. It can be shown that

$$T_c = 2\pi \frac{\alpha_V \dot{u}_{go}}{\alpha_A \ddot{u}_{go}}, \quad T_d = 2\pi \frac{\alpha_D u_{go}}{\alpha_V \dot{u}_{go}} \tag{1}$$

where α_A, α_V, and α_D are the amplification factors for the three spectral regions.

Comparing Figure 7(a) with 7(b) indicates that the velocity-sensitive region for the NR94rrs ground motion (a near-fault record) is much narrower, and its acceleration-sensitive and displacement-sensitive regions are much wider compared to the Taft motion (a far-fault record). There is a twofold explanation. First, the period $T_c = 0.99$ s for the NR94rrs motion is much longer than $T_c = 0.39$ s for the Taft motion, primarily because the $\dot{u}_{go}/\ddot{u}_{go} = 0.20$ for NR94rrs is much larger than $\dot{u}_{go}/\ddot{u}_{go} = 0.08$ for Taft (Table I). Second, the period $T_d = 1.21$ s for the NR94rrs motion is much shorter than $T_d = 6.1$ s for the Taft motion, primarily because the $u_{go}/\dot{u}_{go} = 0.23$ for NR94rrs motion is much smaller than $u_{go}/\dot{u}_{go} = 0.69$ for Taft motion (Table I).

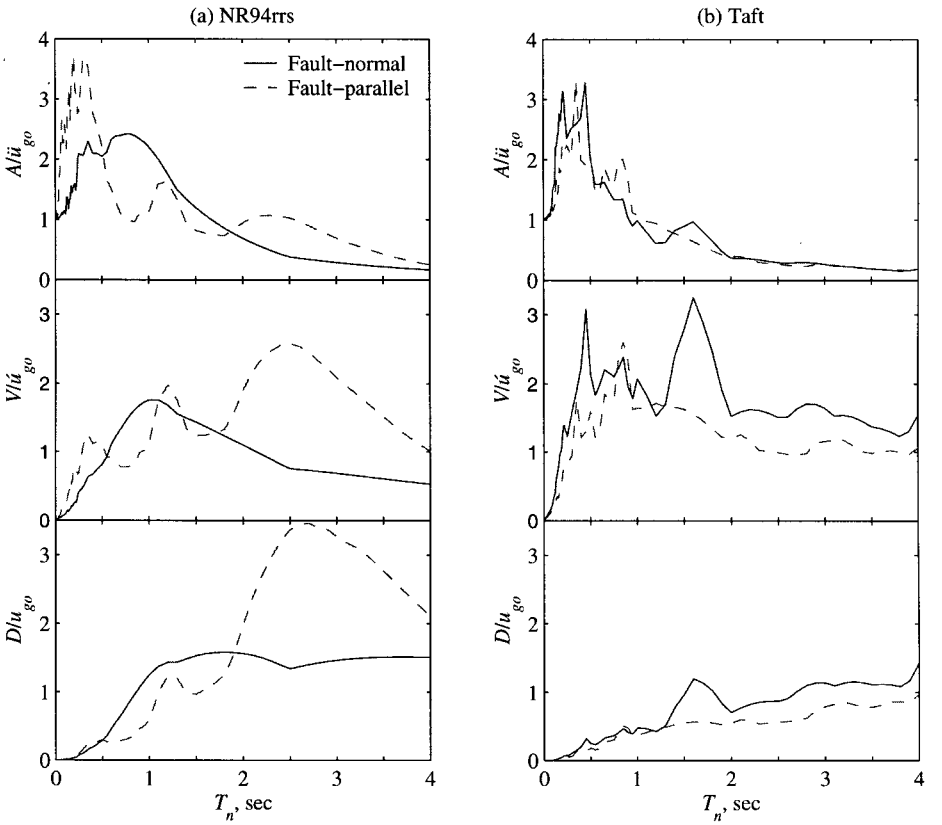

Figure 5. Normalized response spectra for fault-normal and fault-parallel components of (a) NR94rrs and (b) Taft ground motions; damping ratio = 5 per cent.

The narrower velocity-sensitive region—which is shifted to longer periods—and wider acceleration-sensitive and displacement-sensitive regions are characteristic of most near-fault ground motions [3], as shown in Figure 8 where the idealized response spectrum is presented for three near-fault motions. Table I shows clearly that their $\dot{u}_{\mathrm{go}}/\ddot{u}_{\mathrm{go}}$ values are typically much larger and $u_{\mathrm{go}}/\dot{u}_{\mathrm{go}}$ values are much smaller compared to far-fault motions like the Taft record. Some implications of the wider acceleration-sensitive region have been discussed elsewhere [7].

It is worth noting that the amplification factors α_A, α_V and α_D vary among the near-fault ground motions (Table I); however, their coefficients of variation are rather small: 0.20, 0.27 and 0.25, respectively.

Later we will need the T_a, T_b and T_c values that separate the spectral regions of the mean response spectrum for the ensemble of 15 far-fault motions and for the set of 15 near-fault motions. These values were determined by fitting an idealized spectrum to the mean spectrum: $T_a = 0.025$ s, $T_b = 0.22$ s, and $T_c = 0.42$ s for the far-fault ensemble; and $T_a = 0.040$ s, $T_b = 0.35$ s, and $T_c = 0.79$ s for the near-fault ensemble.

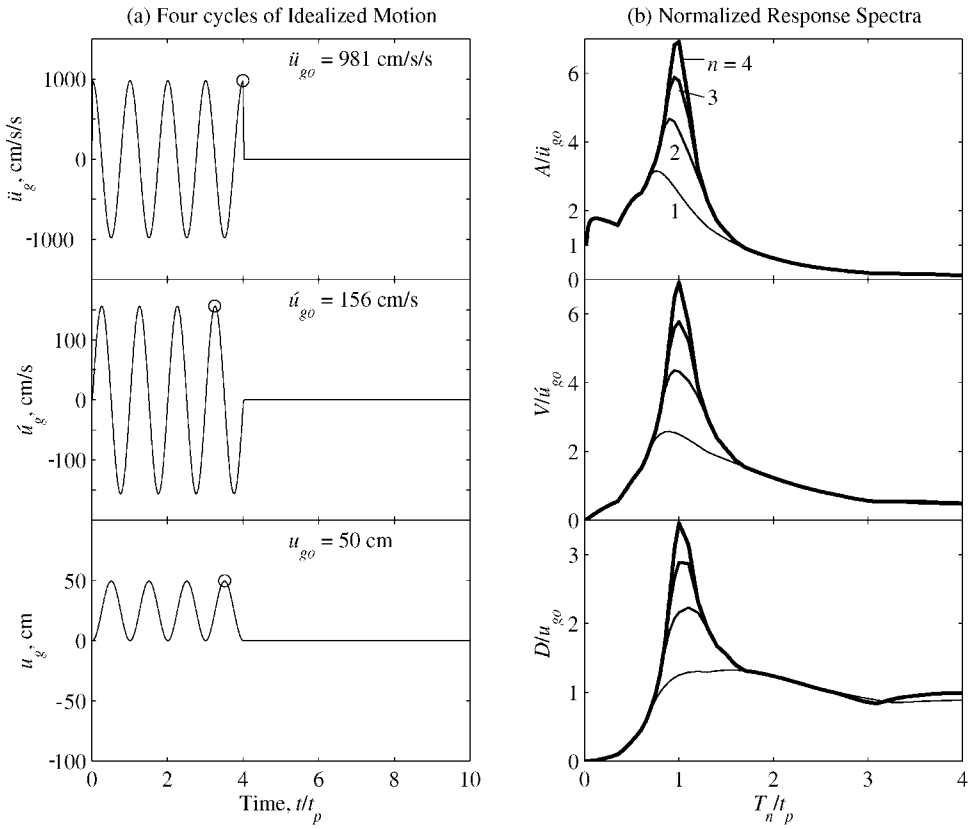

Figure 6. (a) Acceleration, velocity, and displacement describing four cycles of idealized ground motion with period t_p. (b) Normalized response spectra for idealized motion containing n cycles; $n = 1, 2, 3$ and 4.

RESPONSE OF INELASTIC SYSTEMS

It is well known that the yield strength f_y required of an SDF system permitted to undergo inelastic deformation is less than the minimum strength f_0 necessary for the structure to remain elastic. Thus building codes define the design force as the elastic demand divided by the strength reduction factor, $R_y = f_0/f_y$, whose value depends on the ductility factor.

Figure 9(a) presents the R_y for elastoplastic systems with a ductility factor of 4 that was computed for NR94rrs and Taft ground motions, where the T_c value that separates the acceleration- and velocity-sensitive spectral regions has been identified. Similar data are presented in Figure 10(a) for selected ensembles of 15 near-fault (15NF) ground motions in Table I and of the 15 far-fault (15FF) motions mentioned earlier. In addition to the mean values of R_y presented for both sets of excitations, the mean-plus-one-standard-deviation and the mean-minus-one-standard-deviation curves are included for near-fault motions.

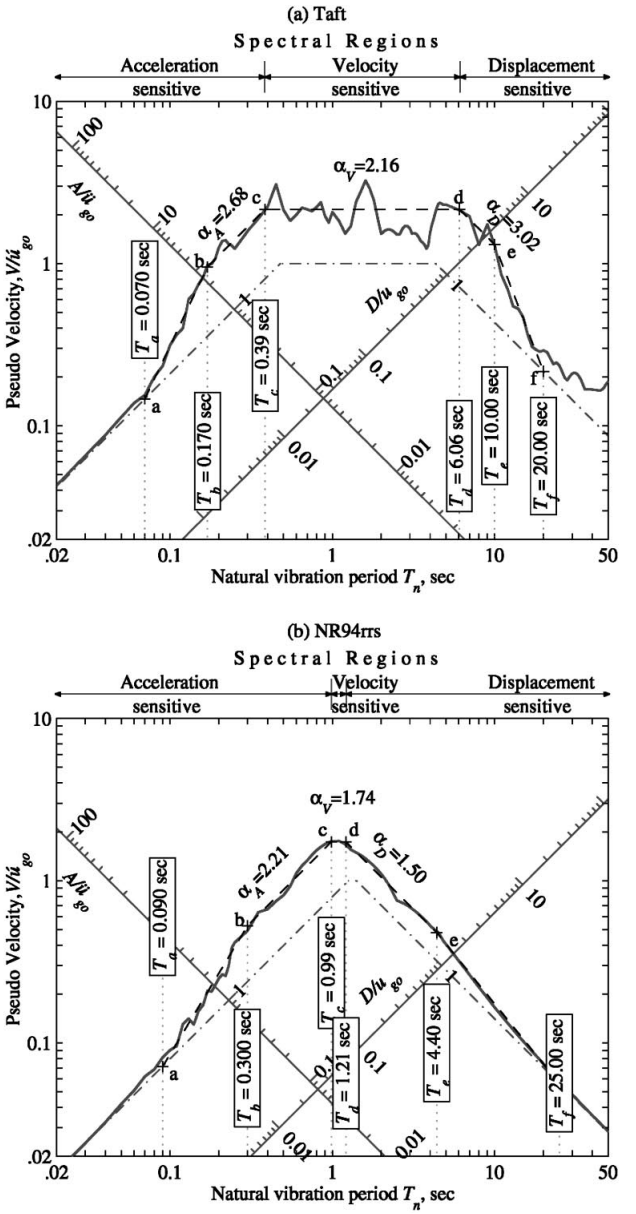

Figure 7. Response spectrum for fault-normal component of (a) Taft and (b) NR94rrs ground motions shown by a solid line together with an idealized version shown by a dashed line; $\zeta = 5$ per cent.

As expected from earlier studies of response to far-fault excitations (e.g., Reference [11, Section 7.7]), Figures 9(a) and 10(a) demonstrate that R_y approaches 1 at very short periods and 4, the ductility factor, at very long periods for both near-fault and far-fault motions. The variation in between is irregular (Figure 9(a)), which is typical of individual ground

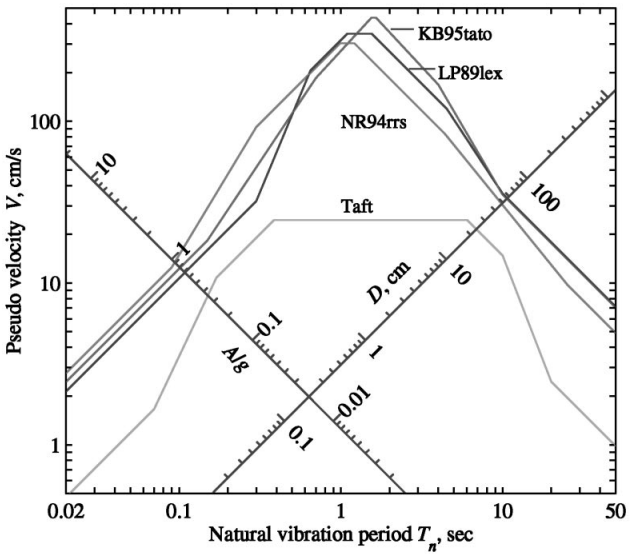

Figure 8. Idealized response spectra for fault-normal component of three near-fault ground motions and of the Taft record; $\zeta = 5$ per cent.

motions, but becomes relatively smooth for the average value over 15 motions (Figure 10(a)). However, in the acceleration-sensitive spectral region ($T_n < T_c$), the strength reduction factor for near-fault motions is systematically and significantly smaller compared to far-fault motions, implying that, for the same ductility factor, near-fault motions impose a larger strength demand compared to far-fault motions, with both demands expressed as a fraction of their respective elastic demands. Such data have led to the concern that existing strength reduction factors, based on far-fault data, may be unconservative for short-period structures.

This systematic difference between the values of the strength reduction factor for near-fault and far-fault motions in the acceleration-sensitive spectral region is primarily due to the difference between the T_c values for the two sets of excitations. This is demonstrated by replotting the R_y data of Figures 9(a) and 10(a) against the normalized vibration period T_n/T_c, as shown in Figures 9(b) and 10(b), respectively. Now the strength reduction factor values for the near-fault and far-fault ground motions are similar in the acceleration-sensitive ($T_n < T_c$) region of the spectrum (Figures 9(b) and 10(b)), and also in the velocity- and displacement-sensitive spectral regions ($T_n > T_c$) if we focus on the average values for both types of motions (Figure 10(b)).

With the increasing emphasis on estimating earthquake-induced deformations in performance-based design, it is of interest to relate the peak deformation u_m of an inelastic system to the peak deformation u_0 of the corresponding elastic system. The ratio u_m/u_0 for NR94rrs and Taft ground motions is presented in Figure 11(a). Similar data are presented in Figure 12(a) for the selected ensembles of 15 near-fault and 15 far-fault ground motions. In addition to the mean values of u_m/u_0 for both sets of excitations, the values that are one standard deviation above and below the mean are also presented for near-fault excitations. As expected [11, Section 7.4.2]. Figures 11(a) and 12(a) demonstrate that for both near-fault and

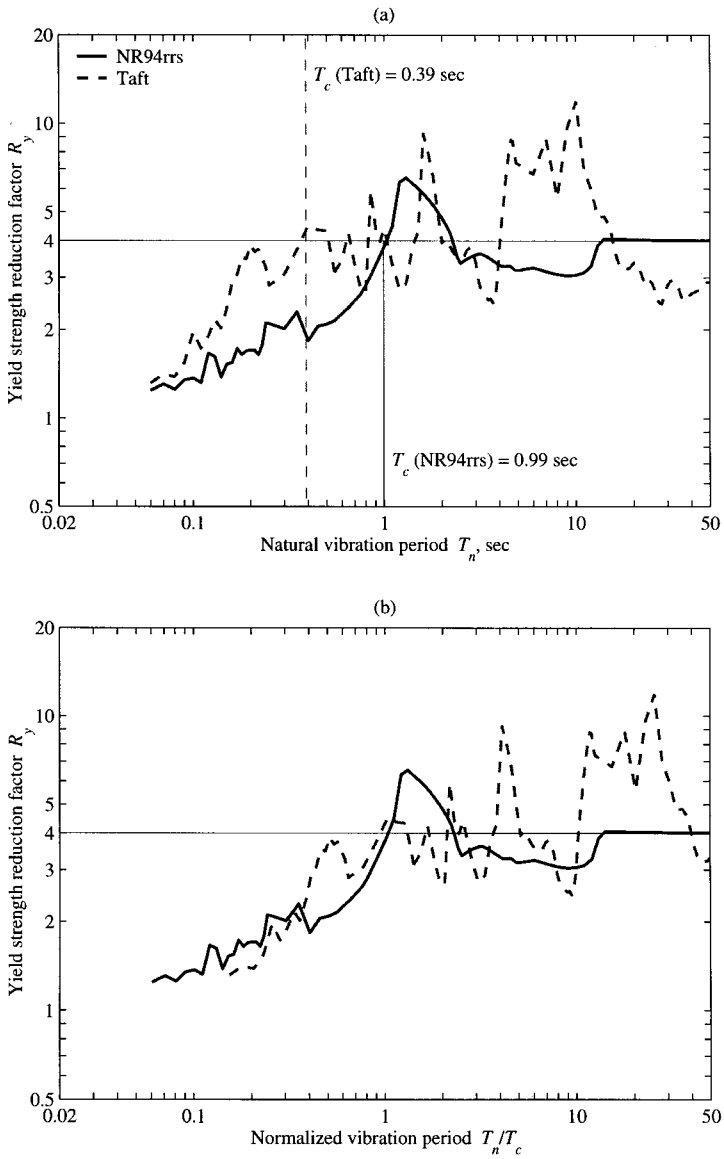

Figure 9. Variation of strength reduction factor with (a) T_n and (b) T_n/T_c for fault-normal component of NR94rrs and Taft records; ductility factor = 4; $\zeta = 5$ per cent.

far-fault excitations u_m/u_0 approaches 1 at very long periods, exceeds 1 in the acceleration-sensitive region of the spectrum ($T_n < T_c$) and approaches the value of the ductility factor for $T_n < T_a$. As expected, the variation of u_m/u_0 with T_n is highly irregular for individual ground motions (Figure 11(a)), but relatively smooth for the average value over 15 motions (Figure 12(a)). However, in the acceleration-sensitive spectral region ($T_n < T_c$), the ratio u_m/u_0 for

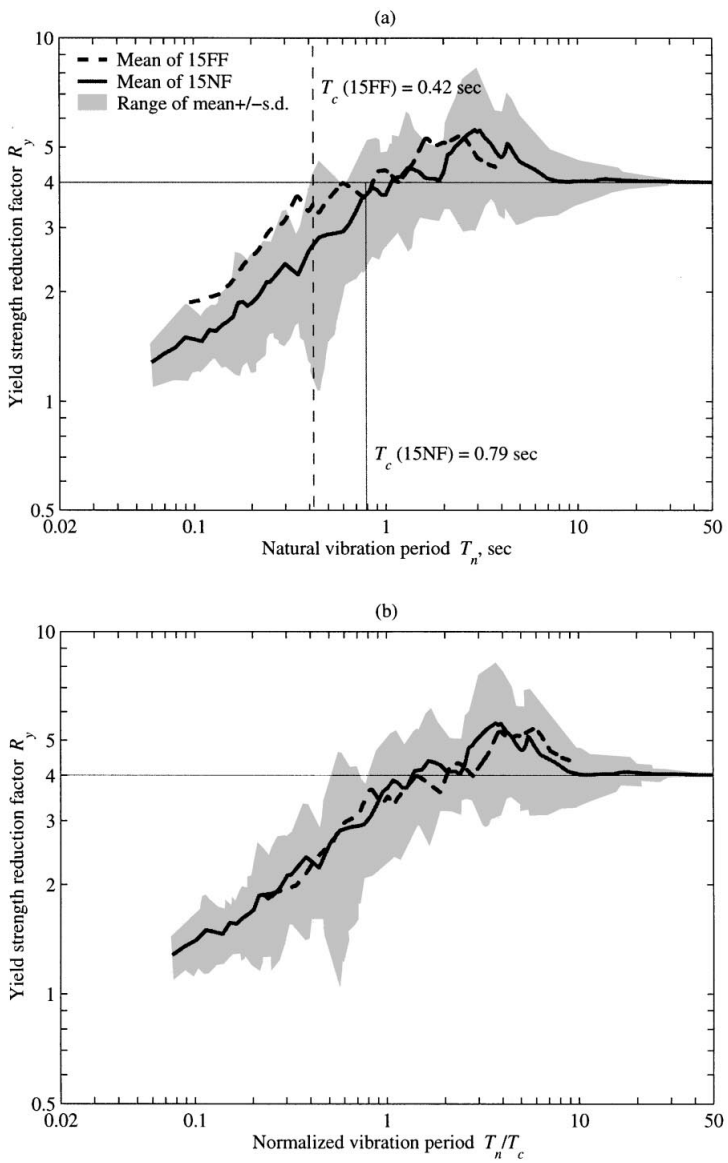

Figure 10. Variation of strength reduction factor with (a) T_n and (b) T_n/T_c for 15 near-fault (15NF) and 15 far-fault (15FF) records; ductility factor = 4; $\zeta = 5$ per cent.

near-fault motions is systematically and significantly larger than its value for far-fault motions. Therefore, the peak deformation of inelastic systems due to near-fault motions would be systematically and significantly underestimated if the u_m/u_0 data from far-fault motions were to be used.

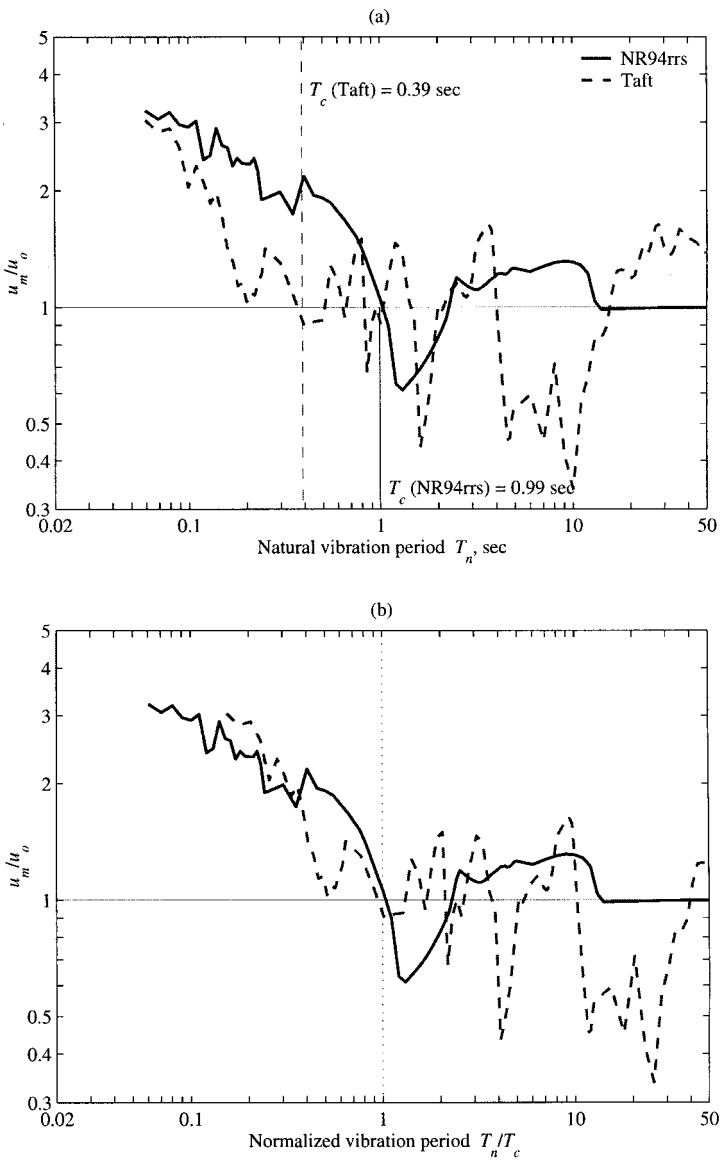

Figure 11. Ratio u_m/u_0 of the peak deformations of elastoplastic systems and corresponding elastic systems due to fault-normal component of NR94rrs and Taft ground motions; plotted against (a) T_n and (b) T_n/T_c; ductility factor = 4; $\zeta = 5$ per cent.

This systematic difference between the values of u_m/u_0 for near-fault and far-fault motions in the acceleration-sensitive spectral region is primarily due to the difference between the period T_c values for the two sets of excitations, which can be demonstrated by replotting the data of Figures 11(a) and 12(a) against the normalized vibration period T_n/T_c, as shown

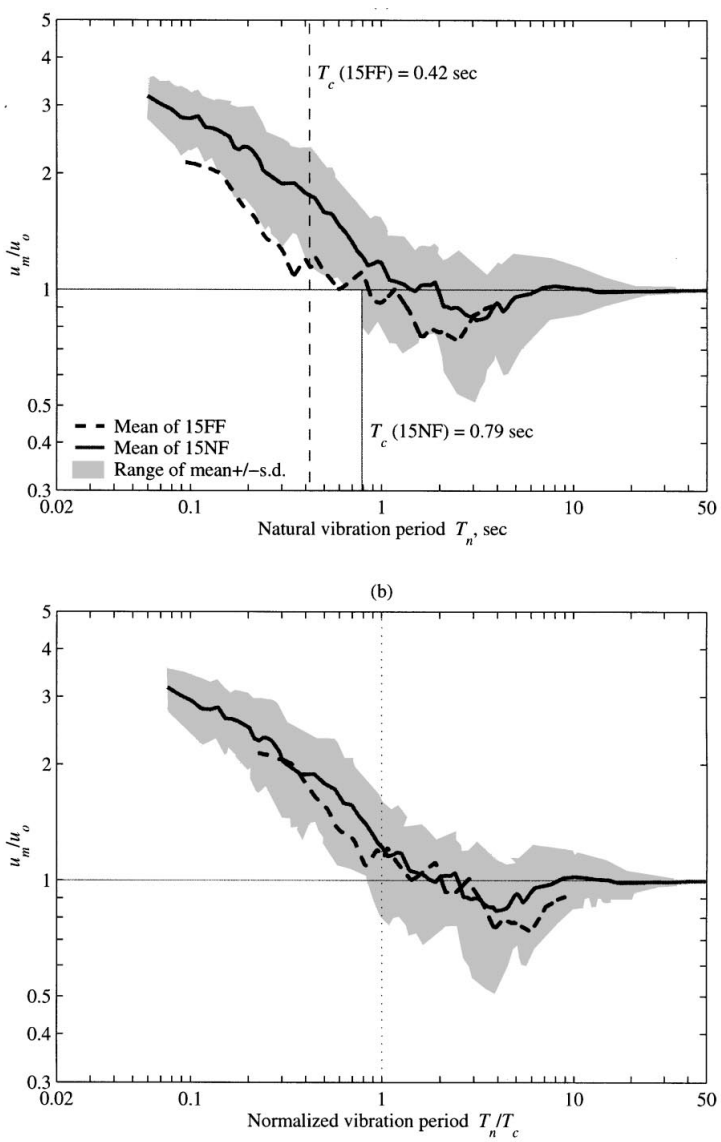

Figure 12. Ratio u_m/u_0 of the peak deformations of elastoplastic systems and corresponding elastic systems due to 15 near-fault (15NF) and 15 far-fault (15FF) records; plotted against (a) T_n and (b) T_n/T_c; ductility factor = 4; $\zeta = 5$ per cent.

in Figures 11(b) and 12(b), respectively. Now the u_m/u_0 values for the near-fault and far-fault ground motions are similar in the acceleration-sensitive ($T_n < T_c$) region of the spectrum (Figures 11(b) and 12(b)), and also in the velocity- and displacement-sensitive spectral regions, $T_n > T_c$, if we focus on the average values for both types of motions (Figure 12(b)).

INELASTIC DESIGN SPECTRUM

A constant-ductility design spectrum is established by dividing the elastic design spectrum by appropriate ductility-dependent reduction factors that depend on T_n. The earliest recommendation for the reduction factor, R_y, goes back to the work of Veletsos and Newmark [12], which is the basis for the inelastic design spectra developed by Newmark and Hall [13]:

$$R_y = \begin{cases} 1, & T_n < T_a \\ \sqrt{2\mu - 1}, & T_b < T_n < T_{c'} \\ \mu, & T_n > T_c \end{cases} \tag{2}$$

where $T_{c'} = (\sqrt{2\mu - 1}/\mu)T_c$. Equation (2) is plotted in Figure 13(a), where the sloping straight lines provide transition among the three constant segments. In recent years, several recommendations for the reduction factor have been developed, some by regression analysis of the data from response history analysis of many SDF systems [8, 14–16].

One of these is defined by Equations (3) and (4) [8]:

$$R_y = [c(\mu - 1) + 1]^{1/c} \tag{3}$$

where

$$c(T_n, \alpha) = \frac{T_n^a}{1 + T_n^a} + \frac{b}{T_n} \tag{4}$$

and the numerical coefficients are $a = 1$ and $b = 0.42$ for elastic–perfect-plastic systems. For a selected R_y-μ-T_n relation, equations can be developed for the ratio u_m/u_0, recognizing that

$$\frac{u_m}{u_0} = \frac{\mu}{R_y} \tag{5}$$

We now compare the computed mean values of R_y and u_m/u_0 for the ensemble of 15 far-fault ground motions with Equations (2) and (3) for R_y and Equation (5) for u_m/u_0. First presented in Figures 10(a) and 12(a), the computed data are shown again in Figure 13, together with the design equations with $T_a = 0.025\,\text{s}$, $T_b = 0.22\,\text{s}$ and $T_c = 0.42\,\text{s}$, which were determined earlier from the average elastic response spectrum for far-fault motions. Both recommendations for the design equations agree reasonably well with the data for most vibration periods. In particular, Equation (2), which was formulated in the 1960s, and is based on then available limited number of earthquake records, is satisfactory for the currently available records of far-fault earthquake motions.

Are Equations (2) and (3) valid for near-fault ground motions? At first glance it may seem that they are not applicable to near-fault ground motions considering that these equations were originally developed for far-fault motions. However, based on the results presented above, they are valid provided values of T_a, T_b and T_c appropriate for near-fault ground motions are used. For Equation (2) this expectation is confirmed by Figure 14, where computed data from Figures 10(a) and 12(a) are presented again together with Equations (2) and (5) using $T_a = 0.04\,\text{s}$, $T_b = 0.35\,\text{s}$ and $T_c = 0.79\,\text{s}$, which were determined earlier from the average elastic response spectrum of near-fault motions. These design equations agree with the computed data for near-fault ground motions as adequately as they did for far-fault motions. We did

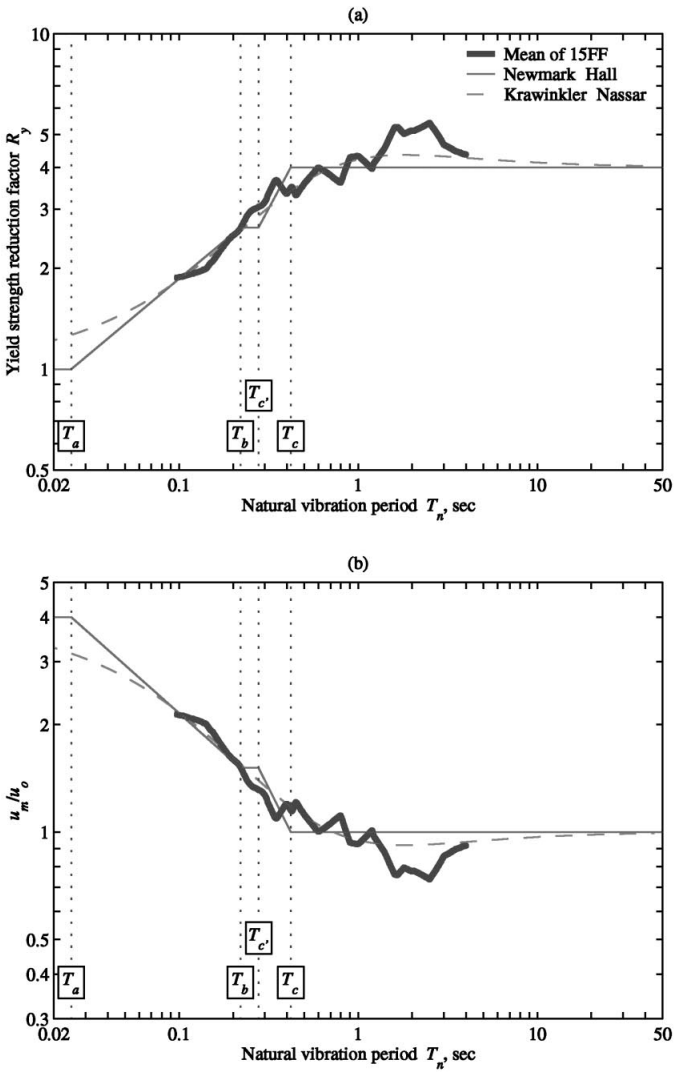

Figure 13. Mean values of (a) strength reduction factor and (b) ratio u_m/u_0 for 15 far-fault (15FF) motions compared with two design equations; ductility factor = 4; $\zeta = 5$ per cent.

not plot the design Equation (3) in Figure 14 because it does not contain T_c and apparently cannot be readily modified for a different T_c value.

The preceding observations and discussion suggest that design equations for R_y (and for u_m/u_0) should explicitly recognize the spectral regions; then the same equation may be applicable to various classes of ground motions—far-fault and near-fault, firm soil and soft soil, smaller magnitude and larger magnitude earthquakes—as long as the appropriate values of T_a, T_b and T_c are used. This requirement is satisfied by Equation (2) but not by Equation (3).

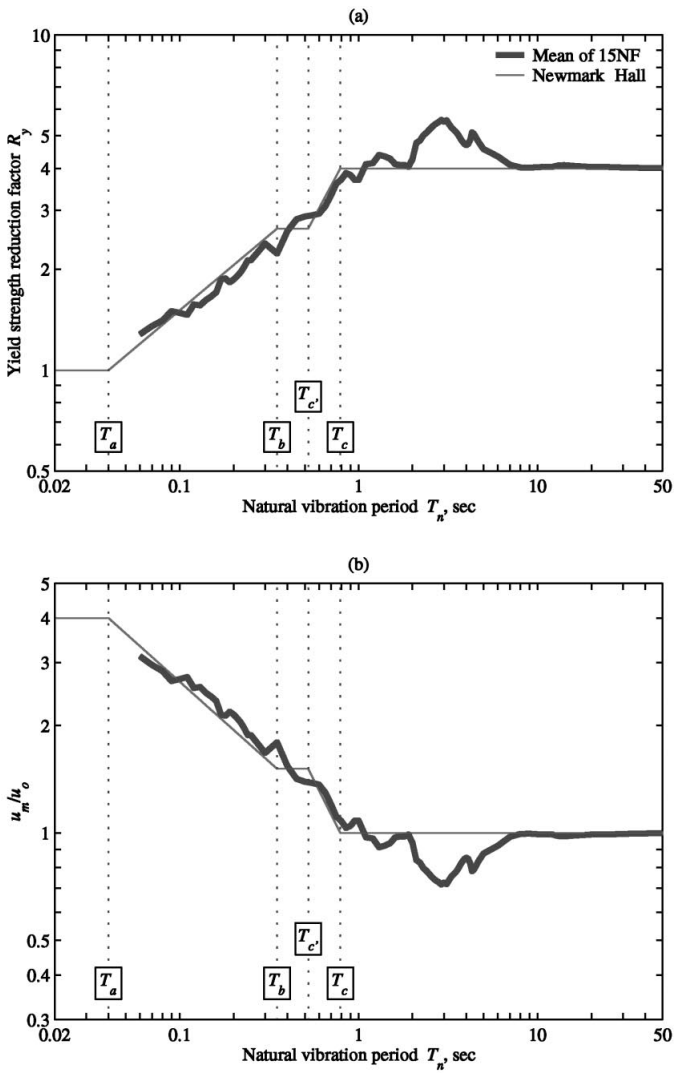

Figure 14. Mean values of (a) strength reduction factor and (b) ratio u_m/u_0 for 15 near-fault (15NF) motions compared with a design equation; ductility factor $= 4$; $\zeta = 5$ per cent.

CONCLUSIONS

This investigation of the response of elastic and inelastic SDF systems has led to the following conclusions:

1. The fault-normal component of many, but not all, near-fault ground motions imposes much larger deformation and strength demands compared to the fault-parallel component

over a wide range of vibration periods. In contrast, the two components of most far-fault records are quite similar in their demands.

2. The strength and deformation demands of the fault-normal component of many near-fault ground motions are much larger than that of the fault-parallel component primarily because the peak acceleration, velocity and displacement of the former are much larger, although its response amplification factors are smaller.
3. The velocity-sensitive spectral region for the fault-normal component of near-fault records is much narrower, and their acceleration-sensitive and displacement-sensitive regions are much wider, compared to far-fault motions. The narrower velocity-sensitive region of near-fault records is shifted to longer periods.
4. For the same ductility factor, near-fault ground motions impose a larger strength demand in their acceleration-sensitive region compared to far-fault motions, with both demands expressed as a fraction of their respective elastic demands. This systematic difference is primarily due to the difference between the T_c values for the two types of excitations. If the period scale is normalized relative to the T_c value, the strength reduction factors for the two types of motions are similar over all spectral regions.
5. In the acceleration-sensitive region the peak deformation of inelastic systems due to near-fault motions would be systematically and significantly underestimated if the u_m/u_0 data from far-fault motions were applied. This difference is primarily a consequence of the different T_c values for the two types of excitations. If the period scale is normalized relative to the T_c value, the u_m/u_0 ratios for the two types of motions are similar over all spectral regions.
6. Design equations for R_y (and for u_m/u_0) should explicitly recognize the spectral regions; then the same equations may be applicable to various classes of ground motions—far-fault and near-fault, firm soil and soft soil, smaller magnitude and larger magnitude earthquakes—as long as the appropriate values of T_a, T_b and T_c are used. In particular, the design equations developed by Veletsos and Newmark in the 1960s with $T_a = 0.04$ s, $T_b = 0.35$ s and $T_c = 0.79$ s are equally valid for the fault-normal component of near-fault ground motions.

ACKNOWLEDGEMENTS

This research investigation is funded by the National Science Foundation under Grant CMS-9812531, a part of the U.S.–Japan Co-operative Research in Urban Earthquake Disaster Mitigation. This financial support is gratefully acknowledged.

REFERENCES

1. Bertero VV, Mahin SA, Herrera RA. A seismic design implications of near-fault San Fernando earthquake records. *Earthquake Engineering and Structural Dynamics* 1978; **6**(1):31–42.
2. Anderson JC, Bertero VV. Uncertainties in establishing design earthquakes. *Journal of Structural Engineering*, ASCE 1987; **113**(8):1709–1724.
3. Hall JF, Heaton TH, Halling MW, Wald DJ. Near-source ground motion and its effects on flexible buildings. *Earthquake Spectra* 1995; **11**(4):569–605.
4. Alavi B, Krawinkler H. Consideration of near-fault ground motions effects in seismic design. *Proceedings of the 12th World Conference on Earthquake Engineering*, New Zealand Society for Earthquake Engineering, Upper Hutt, New Zealand, Paper No. 2665, 2000.

5. Iwan WD, Huang CT, Guyader AC. Important features of the response of inelastic structures to near-field ground motions. *Proceedings of the 12th World Conference on Earthquake Engineering*, New Zealand Society for Earthquake Engineering, Upper Hutt, New Zealand, Paper No. 1740, 2000.
6. Iwan WD. Drift spectrum: measure of demand for earthquake ground motions. *Journal of Structural Engineering*, ASCE 1997; 397–404.
7. Malhotra PK. Response of buildings to near-field pulse-like ground motions. *Earthquake Engineering and Structural Dynamics* 1999; **28**:1309–1326.
8. Krawinkler H, Nassar AA. Seismic design based on ductility and cumulative damage demands and capacities. In *Nonlinear Seismic Analysis and Design of Reinforced Concrete Buildings*, Fajfar P, Krawinkler H (eds). Elsevier Applied Science: New York, 1992.
9. Somerville PG. Development of an improved representation of near-fault ground motions. *SMIP98 Proceedings of the Seminar on Utilization of Strong-Motion Data*, Oakland, California, September 15, California Division of Mines and Geology, Sacramento, 1998; 1–20.
10. Riddell R, Newmark NM. Statistical analysis of the response of nonlinear systems subjected to earthquakes. *Structural Research Series No.* 468, University of Illinois at Urbana-Champaign, Urbana, Illinois, August 1979; 291pp.
11. Chopra AK. *Dynamics of Structures: Theory and Applications to Earthquake Engineering* (2nd edn). Prentice-Hall: Upper Saddle River, NJ, 2001.
12. Veletsos AS, Newmark NM. Effect of inelastic behavior on the response of simple systems to earthquake motions. *Proceedings of the 2nd World Conference on Earthquake Engineering*, Japan, vol. II, 1960; 895–912.
13. Newmark NM, Hall WJ. *Earthquake Spectra and Design*. Earthquake Engineering Research Institute: Berkeley, CA, 1982; 103pp.
14. Vidic T, Fajfar P, Fischinger M. Consistent inelastic design spectra: strength and displacement. *Earthquake Engineering and Structural Dynamics* 1994; **23**(5):507–521.
15. Miranda E, Bertero VV. Evaluation of strength reduction factors for earthquake-resistant design. *Earthquake Spectra* 1994; **10**(2):357–379.
16. Riddell R, Hidalgo PA, Cruz EF. Response modification factors for earthquake resistant design of short period buildings. *Earthquake Spectra* 1989; **5**(3):571–590.

